GNC and ICATT Conference
12-16 June, 2023 | Sopot | Poland

AOCS FINE POINTING TECHNIQUES FOR ESA PLATO MISSION

N. Kutrowski[1]
P. Cruciani[2]
F. Boquet[3]
A. Monsky[4]

[1]Thales Alenia Space, France.
[2]Thales Alenia Space, United Kingdom.
[3]European Space Agency, Netherlands
[4]OHB System AG, Germany

ABSTRACT

Planned for a launch in December 2026, PLATO is the 3rd medium mission of the Cosmic Vision ESA program.

Based on a payload consisting of 26 cameras that will look at transit of exoplanets in front of their stars, the pointing requirements of PLATO are very stringent.

In order to fulfill the required pointing performances, the AOCS is relying on the use of a Fine Guidance System (FGS), which is part of the payload and on different fine pointing techniques, some of which were developed by Thales Alenia Space in the frame of PLATO.

In the first part, the presentation will recall the objectives and constraints of the PLATO mission, while presenting the AOCS main pointing requirements (APE, MPE, PDE, RPE, performance in frequency domain) and the design of this "payload in the loop" AOCS.

In the second part, the different fine pointing techniques will be presented. A focus will be done on the different Kalman filters used for the attitude and angular rates estimation, reaction wheels friction torque estimation, and also how the AOCS is compensating for misalignment between attitude sensors (FGS and Star trackers) and the effect of the kinematic aberration of stars on the FGS line of sight.

1. PLATO MISSION OVERVIEW

PLATO (PLAnetary Transits and Oscillations of stars) is a medium-class astronomical science mission belonging to ESAs Cosmic Vision Programme, which is dedicated to the detection and characterisation of terrestrial exo-planets.
For this purpose, PLATO will be placed in an orbit around the L2 Lagrange point of the Sun-Earth system. By performing long uninterrupted high precision observations of large samples of stars, the planetary transits can be detected and characterised by measuring and analysing the light curves of the stars.
The operational lifetime of PLATO is 6,5 years (including lifetime extension).

1.1. Spacecraft Architecture

The PLATO spacecraft is configured in a modular way, with:

- Payload Module (PLM): contains the full set of instruments, an optical bench, supporting structures and the hardware thermal control. The set of instruments includes twenty-six cameras.
- Service Module (SVM): supports the PLM by providing structural support, command and data management, attitude and orbit control, thermal control, communications, and power generation, conditioning and distribution. The sunshield is considered part of the service module. Also some payload electronic units are accommodated within the SVM.

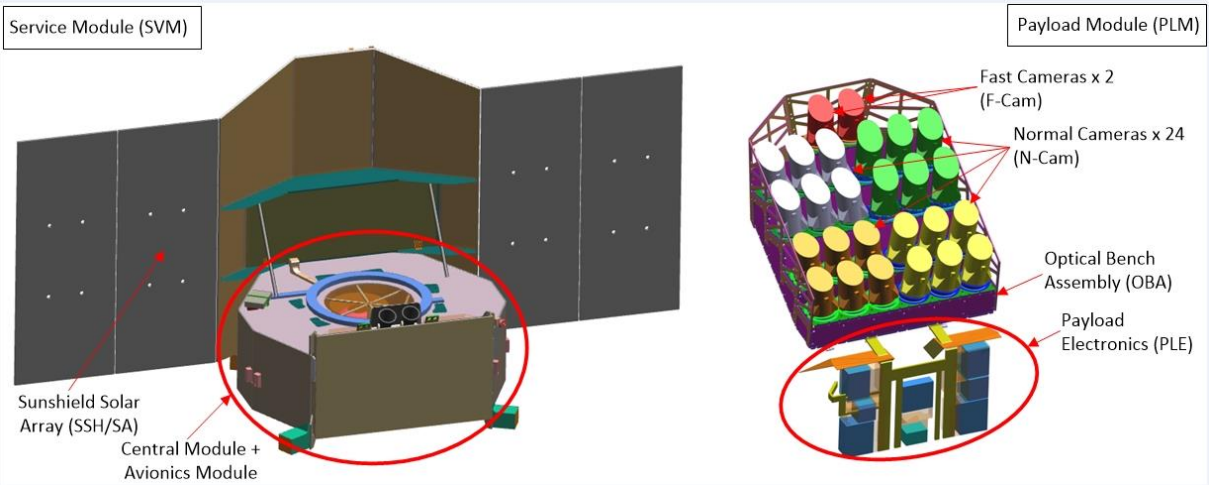

Figure 1: Spacecraft Architecture Overview

In particular, the AOCS subsystem of the satellite has been developed jointly by engineers of Thales Alenia Space in France and Thales Alenia Space in the UK relocated at the Cannes site of the company. The architecture of the avionics as well as of the AOCS are under the responsibility of Thales Alenia Space in France.

1.2. Main mission constraints

From an AOCS prospective, there are two main constraints with respect to the combined boresight axis of the telescopes. During any mission phase the Sun may not enter a prohibited cone around the boresight axis of the FoV in order to protect the telescopes. During the operational orbit the Earth and Moon shall also not enter an undesirable region around the

boresight axis. The description of the different zones is provided in Table 1 and depicted in Figure 2.

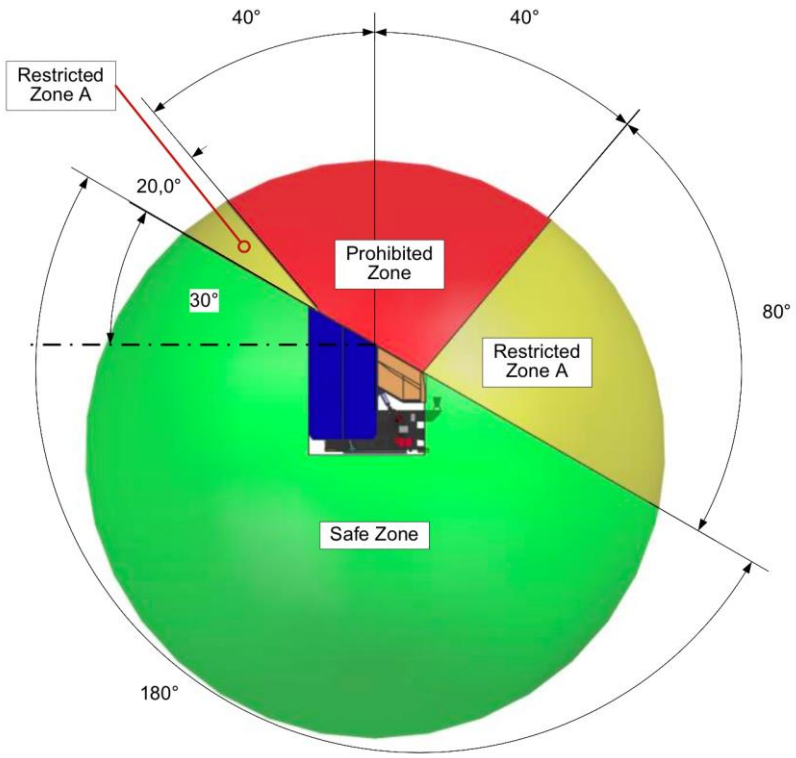

Figure 2: Prohibited, Restricted and Safe zones

Zone	Description
Restricted Zone	A hemisphere tilted by 30 deg about the $y_{S/C}$-axis (refer to Figure 2). In this zone the illumination time by the Sun is limited to 5 min. The restricted zone contains a prohibited zone.
Prohibited Zone	A cone with 40 deg half-cone angle around the LoS which the Sun may never enter
Undesirable Zone	A cone with 30 deg half-cone angle around the LoS which the Earth and Moon should preferably not enter during the operational phase.

Table 1: Description of the Restricted, Prohibited and Undesirable zones

1.3. AOCS modes

The AOCS implements the following modes:

- A Stand-By-Mode (SBM) for AOCS initialization and units status verification on the ground.

- A Safe Mode (SFM) for survival, for sun acquisition and for de-tumbling after launcher separation or other failures provoking residual angular rates. The transition to this mode is possible from all modes, including from SFM itself (mode re-initialization).

- A Guided Attitude Mode (GAM) for medium-accuracy pointing in non-science phases such as quarterly slews, slews to orbit manoeuvers attitude, and in support to micro-scanning activities.

- A Fine Pointing Mode (FPM) for high-accuracy pointing in science phase only. FGS measurements are taken into account is this mode.
- An Orbit Control Mode (OCM) for attitude control during trajectory correction and station keeping manoeuvers.
- An Off-Loading Mode (OLM) for RW angular momentum dumping.

The AOCS modes organization and transitions are depicted in Figure 3.

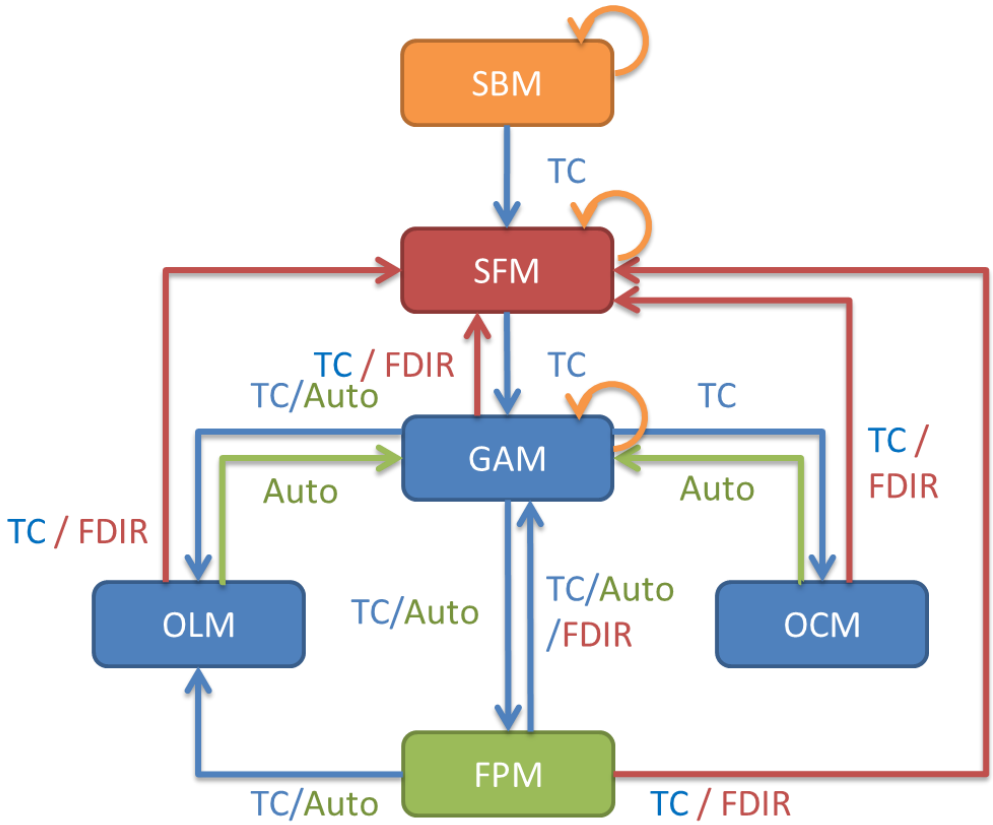

Figure 3: AOCS modes organization and transitions.

1.4. Focus on SFM mode

The Safe mode is decomposed in 3 phases:

- A rate damping phase (Rate Damping Phase - RDP). This phase allows a damping of angular rate close to zero. It is particularly critical at launcher separation where high rates might be created by the launcher. Therefore the RCT are used in order to ensure Sun avoidance constraint.
- A reorientation phase (Sun Pointing Phase - SPP) where the solar array is pointed to the Sun. This phase is performed at a moderate angular rate in order to quickly escape the restricted zone (if inside) but also to reduce propellant consumption.
- An inertial pointing phase (BarBeQueue Phase – BBQ), where the satellite keeps the solar array pointed to the Sun. A small spin could be imposed to the satellite around this axis to provide a better stabilization and to ensure sky survey for STR attitude

acquisition and tracking. A low gain communication antenna has been placed on the same side to enable communications with the ground.

As the only attitude sensor of this mode provides only a direction, it is not possible to obtain a 3 axes stabilized attitude in this mode.

The default actuators for this mode are the Reaction Control Thrusters (RCT). However, in inertial pointing phase, it is possible to switch to reaction wheels for attitude control. This switch is first enabled by a ground TC to ensure the correct state of the reaction wheels. It is also possible to go back to RCT (for RWS desaturation for instance) without restarting the safe mode.
Note that the switch is saved in Safe Guard Memory such that an automatic transition to RWS is possible after entering in Safe Mode again.
Consequently the BBQ phase is split in two sub-phases called BBQ-T and BBQ-R respectively for Thrusters and Reaction wheels attitude control.

Figure 4 provides the organization of the SFM phases and their transitions:

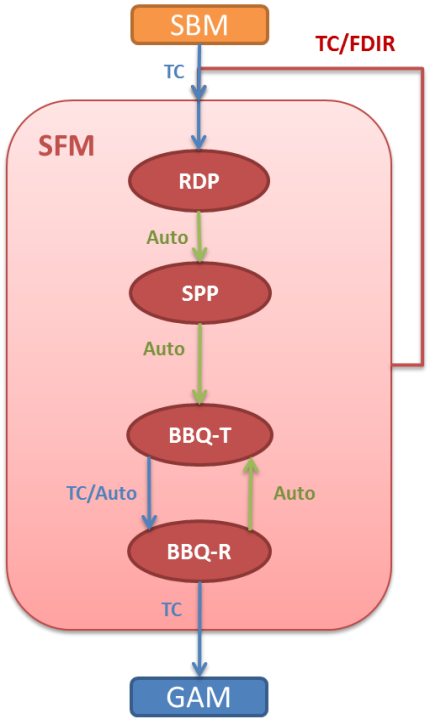

Figure 4: SFM phases organization and transitions

1.5. AOCS equipment

The AOCS is built around the following set of standard sensors and actuators, and the Fine Guidance Sensors provided by the Payload Consortium:

- Attitude and rate sensors for fine pointing operation:
  - 2 Star Tracker (STR) operated in cold redundancy, used for inertial attitude determination in the AOCS modes where Service Module operations take place. It also provides inertial attitude information before transition to the AOCS Fine-Pointing Mode where attitude measurements are provided by the FGS.

- 1 High Performance Gyro (HPG) internally redundant, used for its very accurate rates measurements
- 2 Fine Guidance Sensors (FGS) used for their very precise attitude measurement. The 2 FGS can be used together for the attitude estimation. These sensors are two particular cameras of the payload which have a working frequency ten times faster than the other twenty-four cameras.

- Attitude and rate sensors not directly used for fine pointing:
  - 1 Attitude Anomaly Detector (AAD) internally redundant, used to trigger the Safe Mode when it detects the Sun in its field of view, covering additional 20deg with respect to the sun prohibited zone.
  - 6 Sun Presence Sensors (SPS) internally redundant, used to have an omnidirectional measurement of the sun direction in Safe Mode and Sun Acquisition Mode
  - 2 Coarse Rate Sensors (CRS) operated in cold redundancy, used to have a coarse measurement of the rate in Safe Mode and operated in hot redundancy for rate anomaly monitoring
  - 3 Pressure Transducer (PT) used for tank pressure measurement.
- Actuators:
  - 4 reactions wheels (RW) used for 3 axis fine attitude control. The AOCS uses the 4 wheels in nominal condition but can still work with 3 only in case of failure. The RWA includes a tachometer ring buffer, a pulse counter and a time counter, which stores the time counter values and the speed directions of the wheels for AOCS algorithms processing.
  - 2 branches of 8 Reaction Control Thrusters (RCT) used for attitude control in safe and orbit control mode, mounted in a force-free configuration
  - 2 branches of 2 Orbit Control Thrusters (OCT) used for the realization of delta-V during small or large orbit control manoeuvre.

1.6. Pointing requirements

Table 2 and Table 3 summarize the PLATO pointing requirements:

In FPM mode, the AOCS contribution to the Absolute Pointing Error (APE) of the FGS LoS shall not exceed 2 arcseconds half cone angle, at 99.7% confidence level with ensemble statistical interpretation.
In FPM mode, the AOCS contribution to the Absolute Pointing Error (APE) around the FGS LoS shall not exceed 2 arcseconds at 99.7% confidence level with ensemble statistical interpretation.
In FPM mode, the AOCS contribution to the Pointing Drift Error (PDE) of the FGS LoS shall not exceed 0.3 arcseconds half cone angle over an interval of 3 months.
In FPM mode, the AOCS contribution to the Pointing Drift Error (PDE) around the FGS LoS shall not exceed 0.6 arcseconds over an interval of 3 months.
In FPM mode, the AOCS contribution to the average frequency content of the Mean Pointing Error (MPE) of the FGS LoS shall not exceed the levels specified in the table below over an interval of 12.5 seconds.

In FPM mode, the AOCS contribution to the average frequency content of the Mean Pointing Error (MPE) around the FGS LoS shall not exceed the levels specified in the table below over an interval of 12.5 seconds.
In FPM mode, the maximum amplitude of the AOCS contribution to the Mean Pointing Error (MPE) of the FGS LoS shall not exceed 12 mas RMS.
In FPM mode, the maximum amplitude of the AOCS contribution to the Mean Pointing Error (MPE) around the FGS LoS shall not exceed 26 mas RMS.
In FPM mode, the AOCS contribution to the Relative Pointing Error (RPE) of the FGS LoS shall not exceed 0.16 arcsecond half cone angle over an interval of 2.5 seconds, at 95% confidence level with temporal statistical interpretation.
In FPM mode, the AOCS contribution to the Relative Pointing Error (RPE) around the FGS LoS shall not exceed 0.2 arcsecond over an interval of 2.5 seconds, at 95% confidence level with temporal statistical interpretation.
In FPM mode, the AOCS contribution to the Relative Pointing Error (RPE) of the FGS LoS shall not exceed 0.7 arcsecond half cone angle over an interval of 25 seconds, at 95% confidence level with temporal statistical interpretation.
In FPM mode, the AOCS contribution to the Relative Pointing Error (RPE) around the FGS LoS shall not exceed 1.4 arcsecond over an interval of 25 seconds, at 95% confidence level with temporal statistical interpretation.
During the Point Spread Function (PSF) calibration phase in FPM mode, the AOCS contribution to the Knowledge Drift Error (KDE) of the FGS LoS, obtained on ground after post-processing, shall not exceed 300 mas half cone angle over an interval of 5 seconds, at 95% confidence level with temporal statistical interpretation.
During the Point Spread Function (PSF) calibration phase in FPM mode, the AOCS contribution to the Knowledge Drift Error (KDE) around the FGS LoS, obtained on ground after post-processing, shall not exceed 600 mas half cone angle over an interval of 5 seconds, at 95% confidence level with temporal statistical interpretation.

Table 2: Summary of the PLATO AOCS fine pointing requirements.

Requirement Simplified Description	Value	AOCS Allocation
APE directional at 99.7%	4.5 arcmin	2 arcsec
APE rotational at 99.7%	9 arcmin	2 arcsec
PDE directional over 3 months	3 arcsec	0.3 arcsec
PDE rotational over 3 months	6 arcsec	0.6 arcsec
MPE PSD directional	See Figure 5	See Figure 6
MPE PSD rotational	See Figure 5	See Figure 7
Maximum MPE amplitude RMS directional	12 mas	12 mas
Maximum MPE amplitude RMS rotational	26 mas	26 mas
RPE 2.5s directional at 95%	0.8 arcsec	0.16 arcsec
RPE 2.5s rotational at 95%	1.6 arcsec	0.2 arcsec
RPE 25s directional at 95%	1 arsec	0.7 arcsec
RPE 25s rotational at 95%	2 arcsec	1.4 arcsec
KDE over 5s directional at 95%	300 mas	300 mas
KDE over 5s rotational at 95%	600 mas	600 mas

Table 3. Values of the specifications for the different types of error pointing. Both the system-level value and the AOCS allocation are provided.

For requirements concerning the MPE directional and rotational PSD, the system-level requirement is shown in Figure 5, while the AOCS allocation is provided in Figure 6 and Figure 7.

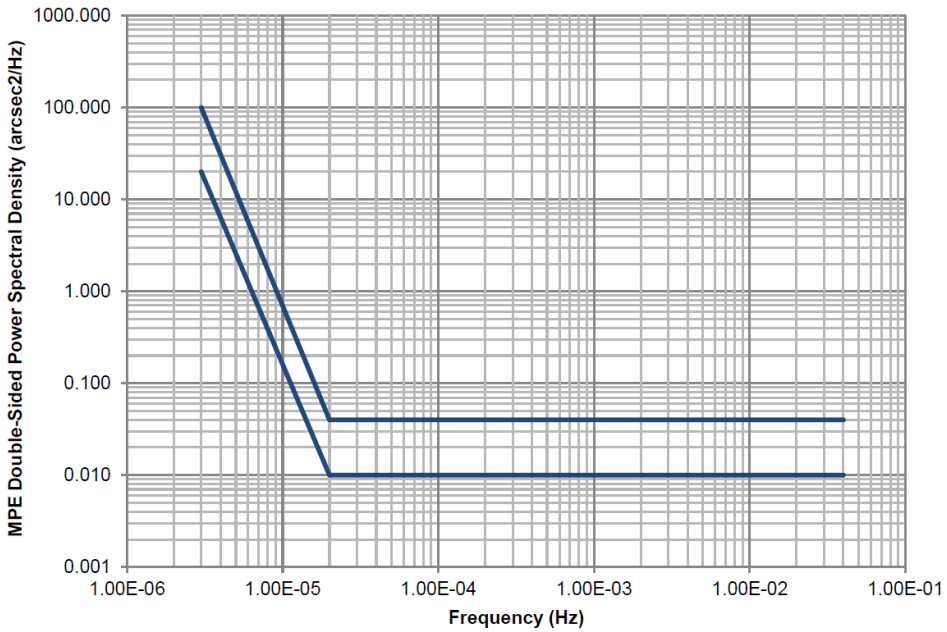

Figure 5: System-level requirement for the MPE double-sided PSD. The upper line is the rotational PSD, while the lower one is the directional PSD.

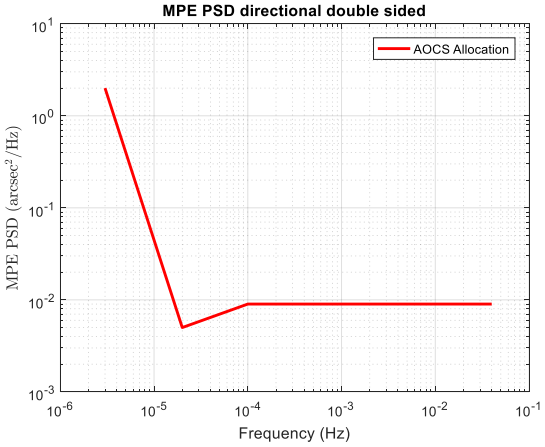

Figure 6: AOCS allocation for directional MPE PSD

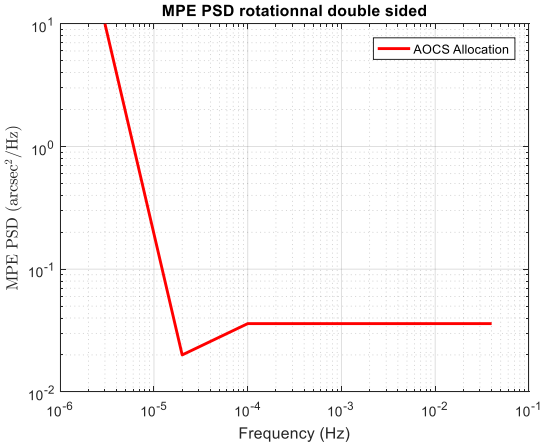

Figure 7: AOCS allocation for rotational MPE PSD

2. FINE POINTING TECHNIQUES

This section shows the different methods employed in order to fulfill the stringent pointing requirements listed in the previous section. In particular, this section focuses on the techniques used to estimate finely the spacecraft attitude and angular velocity, as well as the speed and friction torque of the reaction wheels.

In addition, some onboard algorithms have been developed to guaranty a long term stability by computing and compensating the alignment offsets between the different attitude sensors – i.e. star tracker and FGS, and also the effect of the kinematic aberration of stars on the FGS line of sight.

2.1. Attitude and angular velocity estimation

The attitude and rate estimation relies on a complex Kalman filter which is able to manage:

- S/C angular rate measurements from the HPG.
- S/C attitude measurements from the STR which have one AOCS cycle of delay.
- S/C attitude measurements from one or two FGS with acquisition frequency of 0.4Hz (2.5s period) and a delay up to 3.75s.

In practice, two Kalman Filters (KF) are used in parallel to achieve fine attitude and rate estimation. A first KF (called Rate Kalman Filter) relies on HPG measurement and S/C dynamics equations in order to finely estimate S/C angular rates and provide an estimation of the disturbance torques applied on the S/C which are pre-compensated as part of a feed-forward controller. A second KF (called Attitude Kalman Filter), which is a gyrostellar estimator, relies on the attitude measurement from the FGS or the STR and is used to estimate the S/C attitude and the angular rate bias from the HPG (which is removed from the HPG measurement).

The principle of the rate/attitude Kalman filter is the following: once a new rate/attitude measurement is received, this measurement is compared to the best rate/attitude prediction obtained at the time of the measurement. The difference – also known as innovation – is then used to correct the rate/attitude estimate at that time, and also estimate the disturbance torque / HPG rate bias. The rate at current time is obtained by integrating the different torques involved in the dynamics equations, while the attitude at the current time instant is obtained by propagating all the intermediary attitude with the measured HPG angular velocity (without bias) at each intermediary step, as shown in Figure 8.

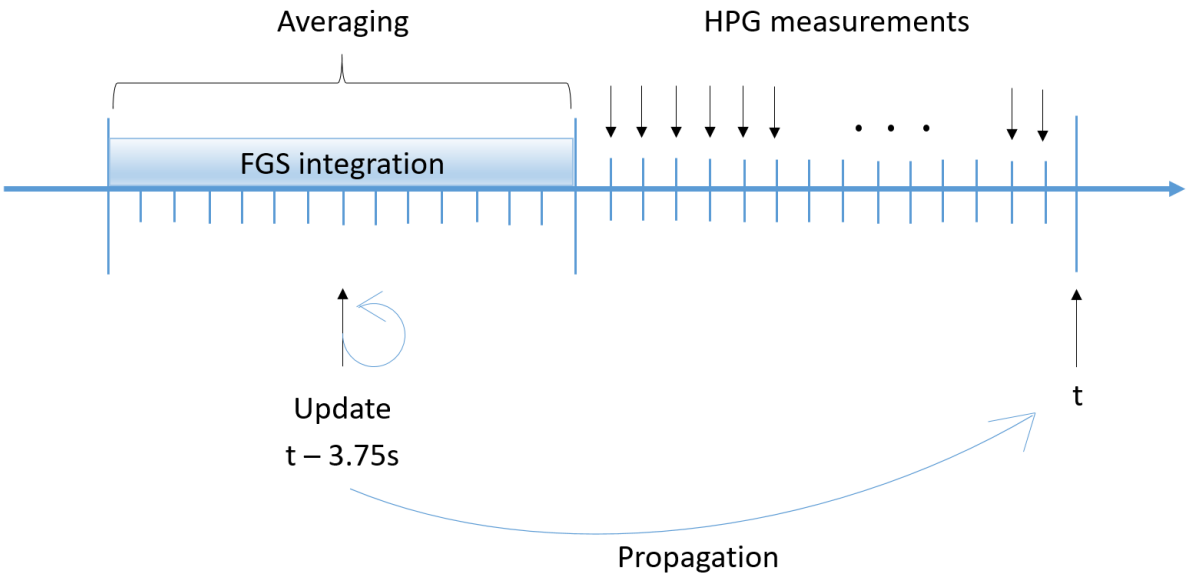

Figure 8. Design concept of the rate/attitude Kalman filter.

In the Fine Pointing Mode (FPM), the FGS measurement are used to feed the Attitude KF. The main challenges are to deal with low sensor frequency (0.4 Hz) compared to the AOCS frequency (8 Hz), a long period of acquisition (2.5s) and a resulting long delay between the middle of the acquisition window and the reception by the AOCS (up to 3.75s).
To tackle these challenges, the AOCS is averaging all the intermediary attitude estimates (produced at 8Hz) along the FGS acquisition window to get the best attitude prediction, and which is consistent with the new attitude measurement. During the "update" step, all the intermediary states up to the current time are updated to get better accuracy during the "propagation" step.

For CPU performance reasons, the use of a filter with a variable gain was not possible. A fixed gain is therefore used with different tuning depending on the set of sensors used.
The Kalman gain values are optimized considering the best knowledge of the sensors' level of noise and the modelling errors.

2.2. RW friction torque estimation

The reaction wheels used on PLATO make use of a twenty-four-pulse tachometer to provide the rate measurement. Moreover, the PLATO spacecraft is fitted with an RTU able to store the time instants at which the tachometer pulses are triggered. This gives a very detailed and high frequency information about the wheel rate which allows a quick estimation of high frequency phenomena such as friction jumps.

The development of the RWS rate and friction estimation algorithms exploited the work performed by Thales Alenia Space as part of the ESA study *Future Enabling AOCS Technologies (FEAT)*[1].

The measured angular rate is then fed to a specific function which estimates the RW friction torque by means of a Kalman filter. The use of this Kalman filter also allows refining the estimation of the RW rate and continue the rate estimation in case of absence or invalid rate measurement. In order to accomplish this, the torque command is also fed to the Kalman filter. Due to the delay between a torque command generation and its realization, the algorithm

considers the commanded torque which is realized during the cycle where tachometer pulses measurements are performed.
This Kalman Filter for RW friction and rate estimation is based on a second order friction model (i.e. including friction derivative as a state) with two possible gains depending on the wheels speed.

The estimated RWS angular speed is later transformed in momentum that is used as a part of the S/C gyroscopic torque estimation. The estimated friction torque is removed from the torque command computed by the controller in order to perform a feed-forward compensation.

2.3. Misalignment computation and compensation

A particular function of the AOCS software is in charge of computing the alignment offsets between all attitude sensors, which are the two STR – the nominal and the redundant one – and the two FGS.

The function computes the error between the two FGS attitude measurements or between one FGS and one STR. A fine measurement synchronization is used to compare attitudes at the same time. Due to the high delay between FGS and STR measurements, and the long FGS acquisition time, when a FGS measurement is received, it is compared with an averaging of all the STR acquisitions performed during the FGS acquisition window, which are kept in memory. The error between the two attitudes is filtered by a cumulative averaging method for a fast convergence of the error. Then, after a defined number of samples, a Kalman filter is used for a smooth moving filtering. The attitude bias estimation is only performed when both sensors data are considered valid and consistent between each other by the AOCS.
An absolute attitude in S/C frame cannot be known due to each unit misalignment (due to mounting error, thermo-elastic deformations, vibrations during launch, …), therefore one of the units is chosen as reference, and the others are corrected with respect to this reference.
The STR attitude (coming from the nominal or redundant unit) is corrected with respect to the FGS attitude. The Ground can select which of the two FGS is considered as the primary one – i.e. the reference. The secondary FGS measurement is corrected with respect to the primary FGS frame.
The correction of the STR attitude measurement allows smooth transitions between FPM (using FGS) and GAM (using STR) modes, and avoid transient due to attitude jumps.
The correction of the secondary FGS attitude measurement allows fusing the measurements of the two FGS, hence improving the attitude estimation accuracy. It also allows a temporary loss of one of the two FGS without interrupting the observations.

2.4. Compensation of the kinematic aberration of stars on the FGS line of sight

Because of the linear velocity the spacecraft has on its orbit, the attitude measurements performed by star sensors – STR and FGS – are affected by the stellar aberration phenomenon. The relative motion of the satellite with respect to the fixed stars causes them to appear displaced towards the direction of motion of the spacecraft for the star sensors. This is shown in Figure 9.

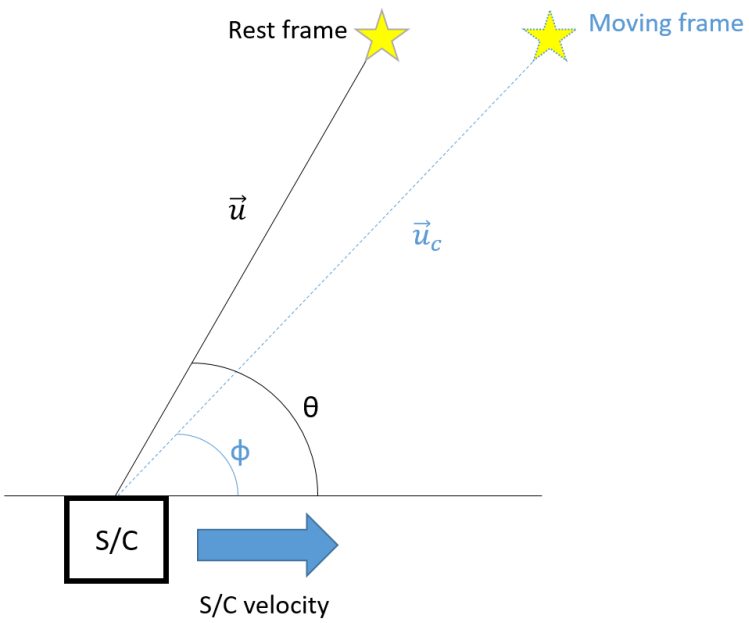

Figure 9. Illustration of the stellar aberration phenomenon. The star is displaced towards the direction of motion of the observer.

This phenomenon must be taken into account in commanding the target attitude of the satellite, which needs to be tilted compared to the same target attitude in a fixed reference frame. This also applies to the star sensors measurements, which need to be corrected to retrieve the actual attitude of the satellite in an inertial frame.

The same compensation algorithm is applied to both the STR and FGS, as shown in Figure 10.

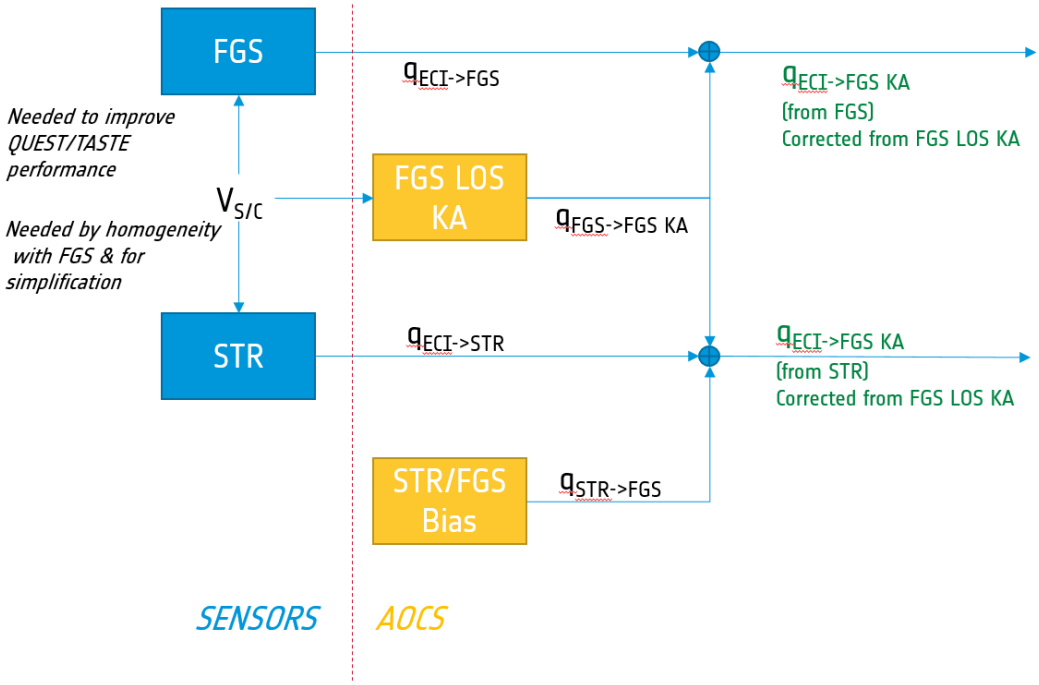

Figure 10: Diagram of how the stellar aberration is compensated by the AOCS software for the FGS and STR measurements.

In order to obtain the star sensor line of sight corrected for stellar aberration, the following algorithm is used. If $\vec{V}$ is the satellite velocity and $\vec{u}$ the star sensor line of sight in the inertial

frame, the line of sight $\vec{u}_c$ corrected for stellar aberration and expressed in the inertial frame can be obtained as follows (also refer to Figure 9):

$$\vec{\beta} = \frac{1}{c} \cdot \vec{V}$$

$$\vec{a} = \left(\vec{\beta} \times \vec{u}\right) \times \vec{u}$$

$$\vec{u}_c = \vec{u} - \vec{a}$$

where c is the speed-of-light constant.

On PLATO, the compensation of the FGS line of sight aberration makes the S/C attitude slightly move along the orbit, reducing the apparent motion of the stars on the FGS CCD captors. This helps to achieve the required long term stability performance.

2.5. Fine pointing simulated performances

Simulations were carried out in order to verify the performances of the AOCS design with respect to the pointing requirements. In particular, a test with degraded unit configurations and worst-case unit noises was carried out to prove the compliance of the design in such conditions.

Figure 11 and Figure 12 show the results obtained for the double-sided MPE directional and rotational PSDs.

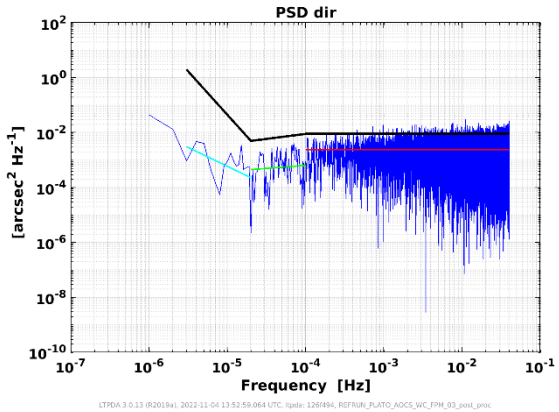

Figure 11: MPE double-sided directional PSD

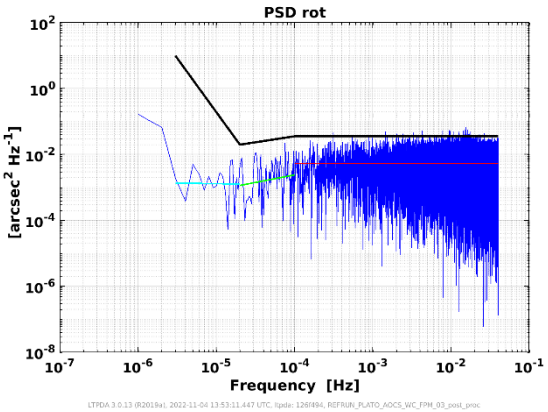

Figure 12: MPE double-sided rotational PSD

An average of the PSDs is calculated in the three main frequency intervals [3e-6Hz, 20e-6Hz], [20e-6Hz, 0.1e-3Hz], [0.1e-3Hz, 2e-1Hz]. This average is compared to the requirement limits and the result proves compliant.

Table 4 also shows the values obtained in this same test for all pointing requirements listed in section 1.6, proving compliance.

Requirement Simplified Description	Requirement value	Obtained result
APE directional at 99.7%	2 [as] (99.7%)	0.609
APE rotational at 99.7%	2 [as] (99.7%)	0.126
PDE directional over 3 months	0.3 [as]	0.085
PDE rotational over 3 months	0.6 [as]	0.159
Maximum MPE amplitude RMS directional	12 [mas]	0.21
Maximum MPE amplitude RMS rotational	26 [mas]	0.32
RPE 2.5s directional at 95%	0.16 [as] (95%)	0.007
RPE 2.5s rotational at 95%	0.2 [as] (95%)	0.007
RPE 25s directional at 95%	0.7 [as] (95%)	0.047
RPE 25s rotational at 95%	1.4 [as] (95%)	0.048
KDE over 5s directional at 95%	300 [mas] (95%)	51.84
KDE over 5s rotational at 95%	600 [mas] (95%)	56.99

Table 4: Summary of the performances obtained in the worst-case scenario compared to the pointing requirements.

3. CONCLUSION

At the time of writing (May 2023) the PLATO project has passed the AOCS CDR.

The AOCS design is completed and the algorithms and tuning have been validated through an extensive robustness/sensitivity Monte-Carlo test campaign on simulator, demonstrating compliance to all the pointing requirements.

The AOCS Software has been generated using automatic code generation process and has been validated at S/W level, and is now under testing on the Avionics Test Bench.

REFERENCES

1. Documents *D5a (Reference spacecraft architecture and specific HW solutions and algorithms*) and *TN1 (Design of a RW state observer*) of the ESA Study *Future Enabling AOCS Technologies (FEAT),* Thales Alenia Space, ESA contract No. 4000116510/16/NL/LF